Observations, Theories, and Predictions of High-Temperature Creep Behavior

B. WILSHIRE

The key observations that have underpinned traditional power-law approaches to creep mechanism identification have been re-evaluated, using information obtained for aluminum, copper, and 0.5Cr0.5Mo0.25V steel. In particular, stress/creep rate plots produced over extended stress ranges for all three materials are shown to be well represented by continuous curves, contradicting the common assumption that different creep mechanisms are dominant over different stress/temperature regimes. Evidence is also introduced to demonstrate that the theoretical and practical limitations of power-law descriptions of steady-state creep rates can be overcome by quantifying the shapes of normal creep curves and the variations in curve shape with changing test conditions. In this way, the behavior patterns displayed by pure metals and particle-hardened alloys can be interpreted in terms of the deformation processes controlling creep-strain accumulation and the damage/degradation processes causing the creep rate to accelerate into the tertiary stages that usually precede fracture. Moreover, the superior predictive capabilities of curve shape analysis are then illustrated by results showing that short-term property values can be extrapolated to provide accurate long-term engineering design data.

I. INTRODUCTION

AT temperatures above about half the absolute melting point (T_m), most metals and alloys exhibit normal creep curves, *i.e.*, following the initial strain on loading, the creep rate decays during the primary stage, reaching a minimum or secondary value before accelerating during the tertiary stage that leads to fracture. Despite this complex curve shape, the creep properties of materials are usually described by reference to the dependences of the minimum creep rate ($\dot{\varepsilon}_m$) on stress (σ), temperature (T), and grain diameter (d) using power-law equations of the form

$$\dot{\varepsilon}_m = A\sigma^n(1/d)^m \exp - Q_c/\mathrm{R}T \qquad [1]$$

where A, n, m, and R are constants, and Q_c is the activation energy for creep. The fact that n, m, and Q_c vary depending on the test conditions imposed is then explained by assuming that different mechanisms, each associated with different vales of n, m, and Q_c, control the creep characteristics displayed within different stress/temperature regimes.

Pure metals are usually considered to show regimes with $n \cong$ one at low stresses and $n \cong 4$ at higher stress levels, with n increasing rapidly in the so-called "power-law breakdown" range, as illustrated by results obtained for aluminum[1–7] in Figure 1. When $n \geq 4$, creep is known to occur by diffusion-controlled generation and movement of lattice dislocations, but no general agreement has been reached on the precise mechanisms involved. Controversy also continues[8–15] over whether creep in the $n \cong$ one regime takes place by diffusional creep mechanisms that do not require dislocation movement (*i.e.*, Nabarro-Herring[16,17] or Coble creep[18]) or by dislocation processes (often referred to as Harper–Dorn creep[2]).

The mechanisms governing creep of pure metals, therefore, remain the subject of unresolved debate, so it is hardly surprising that mechanism identification has proved to be an even more intractable problem with particle-hardened alloys. Yet, the phenomenon of creep has been studied for almost a century, and power-law approaches have been widely adopted to quantify creep behavior patterns for over half a century. For this reason, it seems timely to re-evaluate the key observations providing the foundations for power-law theories, focusing on information obtained for

(a) aluminum and copper, the pure metals most often selected for mechanistic studies; and
(b) 0.5Cr0.5Mo0.25V ferritic steel, a particle-hardened alloy for which extensive data sets are available.

II. CREEP OF ALUMINUM

The creep properties of pure aluminum are not typical of those exhibited by most other pure metals. In particular, during creep at $T \cong 0.5\ T_m$, superpurity aluminum exhibits very large creep strains without the occurrence of necking, and grain-boundary cavities do not form to cause intergranular fracture. Thus, Figure 2 shows a series of creep curves, plotted as creep rate ($\dot{\varepsilon}$) against creep strain (ε), determined at 573 K for superpurity aluminum annealed at 773 K to produce a stable, average grain diameter of 0.25 mm.[19] These tests were carried out in tension using high-precision constant-stress creep machines that incorporated inline load cells verifying that the stress remained constant to within $\pm$0.8 pct over the entire strain range examined. Clearly, under conditions such that recrystallization or grain growth did not occur, in the absence of any damage or degradation process that offsets the decaying primary stage, the creep rate decreased gradually as the creep strain increased towards 0.30.[19] Moreover, under comparable constant-stress test conditions, virtually identical creep curves were recorded

B. WILSHIRE, Professor, is with the Department of Materials Engineering, University of Wales Swansea, Swansea SA2 8PP, United Kingdom.

This article is based on a presentation made in the workshop entitled "Mechanisms of Elevated Temperature Plasticity and Fracture," which was held June 27–29, 2001, in San Diego, CA, concurrent with the 2001 Joint Applied Mechanics and Materials Summer Conference. The workshop was sponsored by Basic Energy Sciences of the United States Department of Energy.

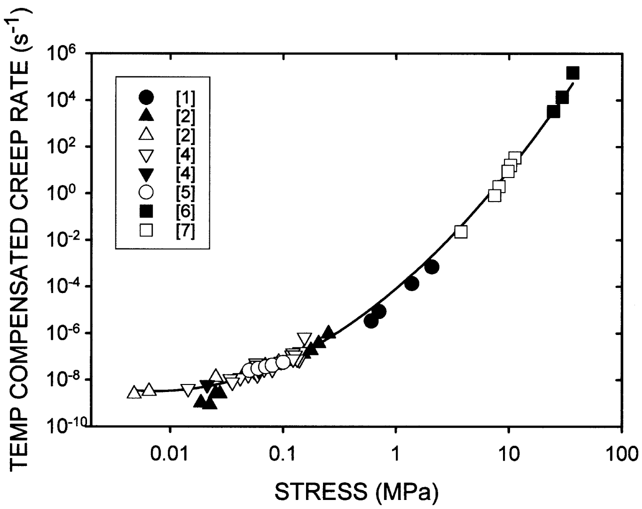

Fig. 1—The stress dependences of the temperature-compensated creep rates determined for single crystals and polycrystalline samples of pure aluminum.[1–7] The results are normalized to 920 K, using an activation energy for creep of 149 kJ mol^{-1}.

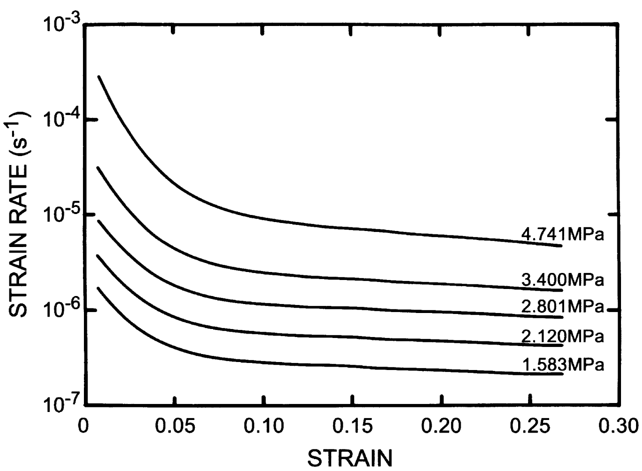

Fig. 2—Constant-stress creep curves, presented to show the variations in creep strain rate ($\dot{\varepsilon}$) with increasing creep strain (ε), determined at stresses from 1.58 to 4.74 MPa at 573 K for pure aluminum having a stable grain diameter of 0.25 mm.[19]

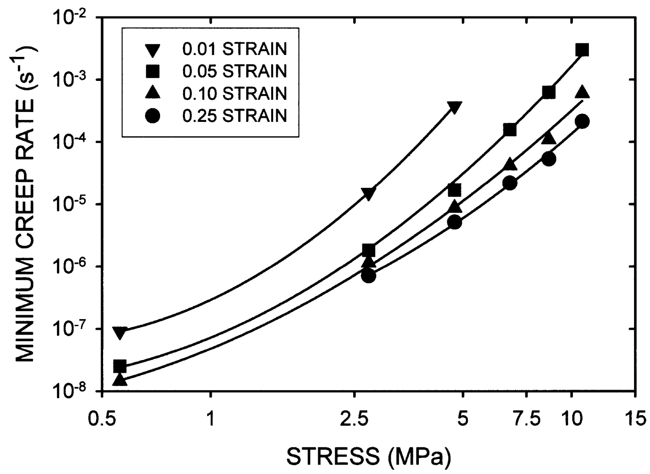

Fig. 3—The stress dependences of the creep rates determined at various creep strains, as derived from the constant-stress creep curves shown in Fig. 2 for pure aluminum at 573 K.

for aluminum single crystals and polycrystals with mean grain diameters of 0.2 and 2.8 mm,[7] a result consistent with the general view that the creep rates observed for aluminum are grain-size independent, *i.e.*, $m = 0$ when $n \geq 4$ (Eq. [1]).

Because the creep rate decays very slowly under constant-stress test conditions, $\dot{\varepsilon}$ may appear to reach a "steady-state" value even after strains of ~0.05, but the actual creep rate continues to decrease with increasing strain (Figure 2). In contrast, using constant-load machines, a "pseudo" secondary stage is reached at relatively low creep strains when the decaying primary rate is offset by the acceleration caused by the progressive reduction in specimen cross-sectional area as the gage length increases. The values shown for $\dot{\varepsilon}_m$ in Figure 1, therefore, depend on the detailed measurement methods adopted by different investigators. Hence, from the $\dot{\varepsilon}/\varepsilon$ curves presented in Figure 2, log σ/log $\dot{\varepsilon}$ plots were constructed for the creep rates displayed at specific creep strains. The results are shown in Figure 3, from which two conclusions can be drawn.

(a) Over any limited stress range, the n value decreases for creep rates measured at higher creep strains, with $n \rightarrow 4$ as $\varepsilon \rightarrow 0.25$ or more.
(b) For creep rates determined at any specific strain, the log σ/log $\dot{\varepsilon}$ plots curve such that n decreases slightly with decreasing stress in the so-called $n \cong 4$ regime.

The results in Figure 3 support the view that all data in Figure 1 can be well represented by a continuous curve. Obviously, this suggestion conflicts with conventional descriptions of log σ/log $\dot{\varepsilon}_m$ plots, which contend that a distinct transition from $n \geq 4$ to $n \cong$ one occurs, as reported in several studies in which the applied stress was decreased to below about 0.1 MPa at 920 K (~0.99 T_m) for aluminum single crystals and polycrystals with grain diameters of 3 to 10 mm.[2–5] Creep of single crystals must occur by dislocation processes because, in the absence of grain boundaries, diffusional mechanisms can make only a trivial contribution to the overall creep rate.

Hence, this evidence led to Harper–Dorn creep being considered as a distinctive dislocation creep process relevant to coarse-grain aluminum and other materials when $n \cong$ one at temperatures near to their melting points. However, on testing five different aluminum samples, including single crystals and polycrystals with $d \cong 4$ to 8 mm, two materials were found to match the Harper–Dorn data, while three materials showed no transition to $n \cong$ one below 0.1 MPa.[20] Three further studies[21,22,23] then reported either no transition to $n \cong$ one or creep rates lower than the Harper–Dorn values.

All of the data sets recorded at stresses below or just above 0.1 MPa are included in Figure 4. Clearly, these results were obtained using aluminum of different purities, produced in different ways. Several different testing methods were adopted, including tension, compression, and double shear, with all experimental systems operating near their lower limit of loading accuracy and strain detection. In addition, definite primary stages were observed in many investigations, but the strains at which the creep rates were measured differed, which would certainly affect the creep rate values quoted in different studies (as indicated in Figure

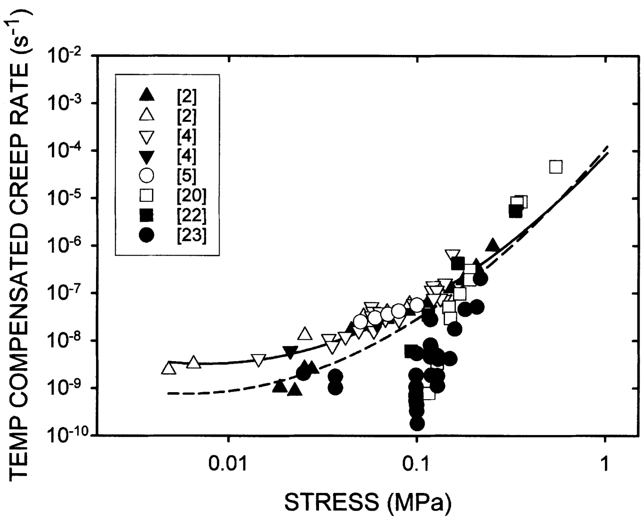

Fig. 4—The stress dependences of the temperature-compensated creep rates recorded at stresses below about one MPa for pure aluminum.[2–5,20,22,23] The results are normalized to 920 K, using an activation energy for creep of 149 kJ mol^{-1}. The solid line was determined using a least-squares curve-fitting routine to describe the data in Fig. 1, whereas the broken line was obtained by applying the same curve fitting procedure to all data in Figs. 1 and 4.

2), especially when much of the data was obtained using stress change tests.

Given the material and test variables involved, the scatter in Figure 4 seems inevitable. Moreover, if all of the data in Figure 4 had been incorporated into Figure 1, very little change would have occurred in the least-squares regression curve shown to fit the results in Figure 1, as illustrated in Figure 4. Because all investigators producing the data in Figures 1 and 4 agree that dislocation creep processes are dominant under all conditions covered, there would then appear to be no justification for the assumption that different dislocation mechanisms are operating in different stress/temperature regimes.

III. CREEP OF COPPER

The results presented in Figure 1 for aluminum show that, over the range of grain diameters covered, the recorded creep rates are grain-size independent. In turn, this observation has underpinned the widely held view that the creep rates are always grain-size insensitive when dislocation creep processes are dominant. Consequently, with copper, the creep rates are generally assumed to be grain-size independent at high stresses (so $m = 0$ when $n \geq 4$), whereas data obtained when $n \cong$ one at low stresses showed that $m = 2$ at 0.82 T_m and $m = 3$ at 0.61 T_m,[24,25] exactly as predicted by diffusional creep theories.

Although the precision of these m value measurements has been challenged,[14] the report that $m \geq 2$ when $n \cong$ one[24,25] has been quoted extensively in support of the contention that diffusional creep mechanisms can govern the creep properties displayed at low stresses. However, the creep properties exhibited by copper have been shown to vary with grain diameter, even when $n \geq 4$ at temperatures around 0.5 T_m.[26] Thus, while the creep rates for copper have been described as grain-size insensitive, a rapid increase in $\dot{\varepsilon}_m$ was noted as d decreased below ~100 μm.[27] Other

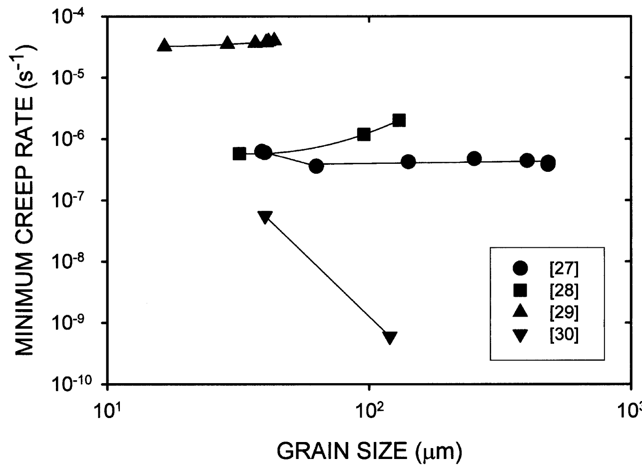

Fig. 5—Grain size dependences of the minimum creep rates recorded for copper.[27–30]

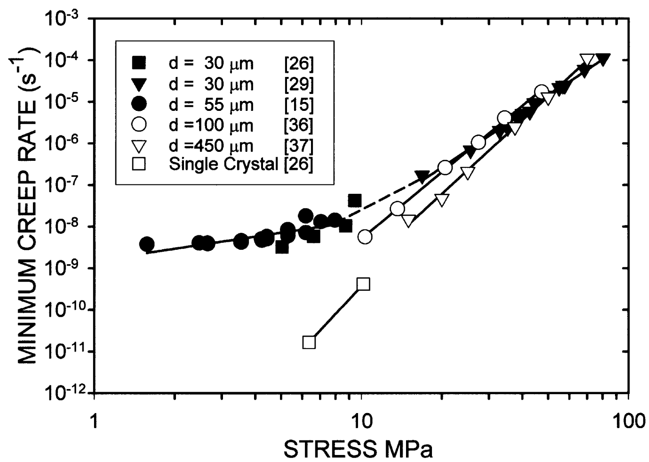

Fig. 6—Stress/minimum creep rate relationships for single crystals and polycrystalline samples of copper produced with different grain diameters. Results are included for $d \cong 30$ μm at 723 K,[29] $d \cong 100$ μm at 728 K,[36] $d \cong 450$ μm at 723 K,[37] and $d \cong 55$ μm at 753 K,[15] together with data for single crystals and polycrystals with $d \cong 30$ μm at 728 K.[26]

studies have then found that $\dot{\varepsilon}_m$ may increase[28] or decrease[29,30] with decreasing grain diameter (Figure 5).

The seemingly conflicting results shown for copper in Figure 5 can be rationalized on the basis that, for many metals and alloys,[31–35] a minimum in the $d/\dot{\varepsilon}_m$ plots occurs at a specific grain diameter ($d_{\min}$), which varies as the test conditions are altered. This dependence of $d_{\min}$ on test conditions then implies that the gradients (n) of log σ/log $\dot{\varepsilon}_m$ plots can be grain-size dependent, as verified for copper in Figure 6. Hence, n values of 4.3, 5.3, and 5.9 were observed at stresses from ~20 to ~80 MPa at ~723 K for copper with mean grain diameters of about 30,[29] 100,[36] and 450 μm,[37] respectively, with $n \cong 6.6$ for single crystals at 7 to 10 MPa.[26] Clearly, these log σ/log $\dot{\varepsilon}_m$ plots intersect so that, for copper at stresses above or just below the yield stress at 723 K (~50 MPa), a minimum can occur in the $d/\dot{\varepsilon}_m$ relationships, accounting for the dependences of $\dot{\varepsilon}_m$ on d changing as the grain-size range the test conditions are varied in the $n \geq 4$ regime (Figure 5). The results in Figure 6 also reveal that $d_{\min}$ increases with decreasing stress such that,

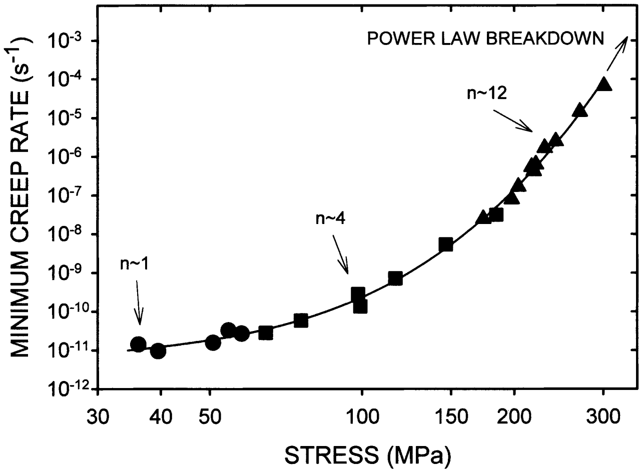

Fig. 7—The stress dependence of the minimum creep rates recorded for 0.5Cr0.5Mo0.25V steel at 838 K. The solid line was computed from the data obtained at stresses of ~200 MPa and above, with the accuracy of the extrapolation confirmed by independent measurements obtained at ~200 MPa and below.[38]

for all grain sizes considered, $\dot{\varepsilon}_m$ increases with decreasing grain diameter at stresses below ~20 MPa.

Interestingly, the data at ~723 K for copper with $d \cong 30$ μm obtained at stresses from ~80 to 20 MPa[29] and ~10 to 5 MPa[26] coincide extremely well with results at 753 K for $d \cong 55$ μm at stresses from ~8 to 1.5 MPa,[15] indicating that the grain-size difference compensates almost exactly for the difference in test temperature (Figure 6). Thus, the log σ/log $\dot{\varepsilon}_m$ plot for $d \cong 30$ to 55 μm shows that n decreases towards $n \cong$ one with decreasing applied stress, with a corresponding transition to $n \cong$ one expected for the larger grain diameters, albeit at lower creep rates. Yet, while it is accepted that dislocation processes are dominant as n decreases towards 3, the transition to $n \cong$ one has been attributed to a change from dislocation to diffusional creep mechanisms,[15] even though the measured creep rates in the $n \cong$ one regime are over an order of magnitude faster that the rates predicted by diffusional creep theories. However, the transition from $n > 3$ to $n \cong$ one is not accompanied by a sudden change from $m = 0$ to $m \geq 2$. Instead, because the creep rates are obviously grain-size sensitive when $n \geq 3$, m progressively approaches 2 or more as n approaches unity (Figure 6). On this basis, there is no need to invoke a change in mechanism as $n \rightarrow$ one , because all features of the behavior patterns displayed in Figure 6 are compatible with dislocation processes being dominant for all grain sizes and test conditions covered.

IV. CREEP OF 0.5Cr0.5Mo0.25V STEEL

Unlike the log σ/log $\dot{\varepsilon}_m$ plots for pure metals (Figures 1 and 6), particle-hardened alloys are widely considered to exhibit regimes not only with $n \cong$ one and $n \cong 4$ but also with $n \gg 4$ before power-law breakdown occurs, as shown for 0.5Cr0.5Mo0.25V steel in Figure 7.[38] Again, no agreed explanation has yet been provided for the very large values of n ($\gg$4) recorded at high stresses for alloys strengthened by dispersions of fine precipitates or insoluble particles. Moreover, Q_c increases as n increases, usually attaining values substantially greater than the activation energies for matrix diffusion when $n \gg 4$.

An early attempt to rationalize these large n and Q_c values suggested[39] that creep occurs not under the full applied stress (σ) but under a reduced stress ($\sigma - \sigma_0$). With the σ_0 approach, the stress and temperature dependences of the creep rate can be written as

$$\dot{\varepsilon}_m = A^*(\sigma - \sigma_0)^p \exp - Q_c^*/\mathrm{R}T \qquad [2]$$

where $A^* \neq A$, $p \cong 4$, and Q_c^* is the creep activation energy derived at constant ($\sigma - \sigma_0$) rather than at constant σ, as in the determination of Q_c (Eq. [1]). In relation to Eqs. [1] and [2] $n \cong p \cong 4$ and $Q_c \cong Q_c^*$ when $\sigma_0 \cong 0$ or when $\sigma_0 \propto \sigma$, whereas $n > p$ and $Q_c > Q_c^*$ when σ_0 is large and decreases with increasing temperature.[40] This idea has been modified and extended considerably over recent decades, with σ_0 now almost universally referred to as a "threshold stress." However, σ_0 cannot be measured reliably or predicted theoretically, so interpretation of the complex creep behavior patterns observed in the $n \geq 4$ regimes for particle-strengthened alloys remains unresolved.[41]

As with pure metals (Figures 1 and 6), a smooth transition from $n \geq 4$ to $n \cong$ one also occurs with 0.5Cr0.5Mo0.25V steel at low stresses (Figure 7), but this transition cannot be explained by existing diffusional creep theories. In the $n \cong$ one range, while the creep rates are usually slower than the measured $\dot{\varepsilon}_m$ values with pure metals, the predicted rates are markedly faster than the observed $\dot{\varepsilon}_m$ data for alloys containing even very small volume fractions of particles.[4] It is then generally claimed that the particle dispersions inhibit vacancy generation and annihilation at grain boundaries, but current diffusional theories have not been modified to provide estimates of the creep rates displayed at low stresses with particle-hardened alloys.

As with the log σ/log $\dot{\varepsilon}_m$ plots for aluminum (Figure 1) and copper with $d \cong 30$ to 55 μm (Figure 6), the results presented in Figure 7 can be well represented by a continuous curve, *i.e.*, n increases gradually rather than in a series of sequential steps from $n \cong$ one, $n \cong 4$, and $n \gg 4$ as different mechanisms are assumed to become dominant with increasing stress. This view is supported by the fact that, for 0.5Cr0.5Mo0.25V steel, comparable dislocation substructures are developed during creep at all stress levels covered in Figure 7, albeit with the dislocation density increasing with increasing applied stress.[38] These observations again suggest that the dislocation processes controlling creep are essentially the same over the entire stress range studied, independent of the n value displayed.

V. STRESS CHANGE EXPERIMENTS DURING CREEP

Information on the dislocation processes occurring during creep can be derived from stress change experiments, following the seminal studies of Nix and co-workers.[42,43] Essentially, when the applied stress (σ) is decreased to a lower value (σ_R), the subsequent creep strain/time behavior depends on whether σ_R is above or below a critical value (σ_i). For $\sigma_R > \sigma_i$, a new positive creep rate is observed, whereas, for $\sigma_R < \sigma_i$, a negative rate is recorded immediately after the stress reduction. These observations reveal that the local internal stress opposing continued movement of a dislocation depends on its position with respect to the other dislocations present. Hence, immediately after a stress

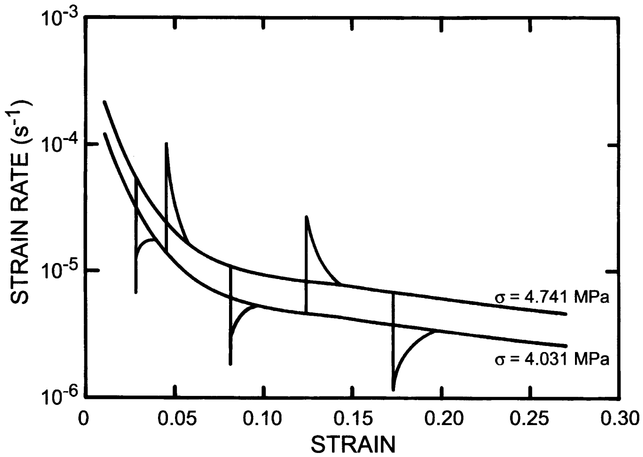

Fig. 8—Strain rate/strain curves recorded for aluminum in constant-stress tests and stress change tests at 573 K.[19]

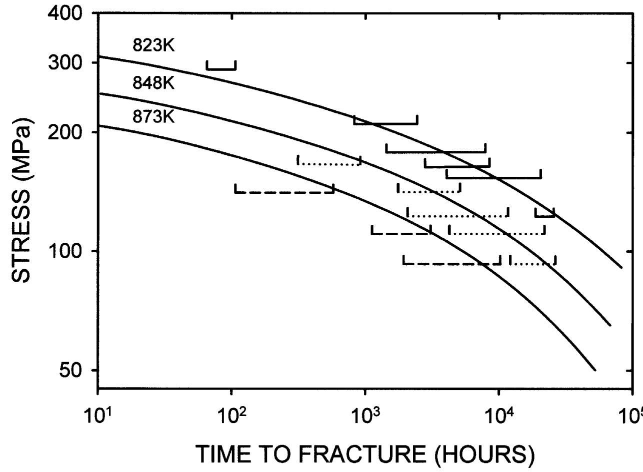

Fig. 9—Stress rupture behavior of 0.5Cr0.5Mo0.25V steel at 823, 848, and 873 K. The solid lines were predicted from tests carried out at stresses giving maximum creep lives of around 1500 h, with the error bars representing multilaboratory test data recorded at these temperatures.[19]

decrease, the new creep rate depends on ($\sigma_R - \sigma_i$), where σ_i is the average internal stress prior to the stress reduction.

Figure 8 illustrates the response to stress changes both up and down between 4.74 and 4.03 MPa at 573 K for superpurity aluminum, presented as $\dot{\varepsilon}/\varepsilon$ plots for tests having durations of ~45 ks.[19] Clearly, the creep strain rate immediately after a stress reduction was always much lower than that which would have been obtained at the same strain during a test conducted wholly at the lower stress. Conversely, the strain rate after a stress increase was always much greater than the rate expected for a test at the higher stress level. However, the creep rates recorded directly after the stress increases and decreases changed progressively towards the rates expected for the new conditions, indicating that the dislocation substructures adjusted gradually to the configurations appropriate to the strains attained under the new stress. Even so, it is important to note that creep strains of the order of 2 pct had to accumulate before the creep rates after the stress changes approached the values anticipated under the new test conditions.

The basic patterns of behavior shown in Figure 8 for aluminum are also followed with copper, although the acceleration of the low creep rates recorded after stress reductions can merge into the tertiary acceleration associated with the development of grain-boundary cavities. These observations indicate that, with pure metals, the dislocation configurations existing at one stress level change only slowly with strain and time after a stress change. In contrast, with materials such as 0.5Cr0.5Mo0.25V steel, the new creep rates measured immediately after stress changes adjust rapidly to the rates expected for the new conditions. This suggests that, while dislocation/dislocation interactions are important with pure metals, dislocation/particle interactions are also relevant with particle-hardened alloys.

When creep is known to occur by diffusion-controlled generation and movement of dislocations when $n \geq 4$ with aluminum, as the primary creep strain accumulates, a well-formed subgrain boundary structure is developed, with a three-dimensional (3-D) network of dislocations within the subcells. Many dislocation theories proposed to explain creep behavior can then be classified into two broad categories depending on whether subgrain boundaries are regarded as vital.[44] However, the idea that creep is determined by low-angle subgrain boundaries seems unlikely when the presence of high-angle grain boundaries has minimal effect on the creep curves recorded for single crystals and polycrystalline samples of aluminum. Moreover, a well-developed subgrain structure is not always formed when $n \geq 4$ at temperatures around 0.5 T_m. Thus, with copper, regions with a 3-D network of dislocations can be surrounded by loose tangles of dislocations and poorly formed subgrain boundaries. Moreover, with particle-hardened alloys, many dislocations are associated with or held up at particles. Hence, dislocation creep theories reliant on the presence of specific dislocation configurations would appear to be of limited value.

VI. INTER-RELATION OF CREEP AND FRACTURE

While continuously decaying curves are observed in constant-stress tests with aluminum (Figure 2), most materials, such as polycrystalline copper and 0.5Cr0.5Mo0.25V ferritic steel, display normal creep curves. For this type of material, the creep rupture life (t_f) often depends inversely on the minimum creep rate as

$$\dot{\varepsilon}_m \cdot t_f = \text{constant} \tag{3}$$

so the nonlinearity of log σ/log $\dot{\varepsilon}_m$ relationships is reflected in log σ/log t_f plots, as illustrated in Figures 7 and 9 for 0.5Cr0.5Mo0.25V steel.[19] This nonlinearity of log σ/log $\dot{\varepsilon}_m$ and log σ/log t_f plots has serious practical implications. For safe and economic design of engineering components subject to creep loading, it is necessary to know the stresses that the relevant materials can sustain under the imposed service conditions:

(a) without reaching some limiting creep strain, or, more usually,
(b) without failure occurring within the planned design lives.

For many applications, design lives can be up to 250,000 hours (over 30 years), so reliable procedures are needed to

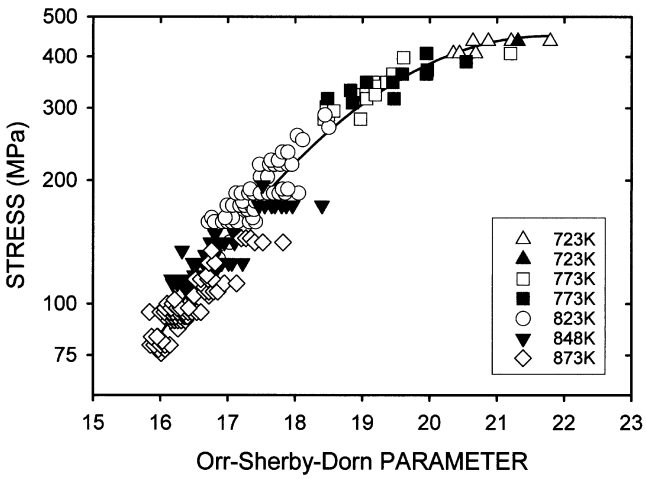

Fig. 10—Stress rupture data for 0.5Cr0.5Mo0.25V steel, showing that data obtained at temperatures from 723 to 873 K can be superimposed onto a master curve using the parametric relationship proposed by Orr *et al.*[45]

allow results obtained in tests of relatively short duration to be extrapolated to provide long-term property estimates. Unfortunately, because of the deficiencies of current theories, extrapolation is undertaken using "parametric" procedures, *i.e.*, empirical methods of plotting stress rupture data using a "correlation parameter" that permits t_f values obtained over a range of temperatures to be superimposed onto a single master curve. For example, the time-temperature parameter (P_{OSD}) introduced by Orr *et al.*[45] is

$$P_{OSD} = \log t_f - (P/T) \qquad [4]$$

where P is a constant selected to fit the data. However, Eq. [4] can be derived simply from Eqs. 1 and 3. Consequently, the curvatures of log σ/log $\dot{\varepsilon}_m$ and log σ/log t_f plots are not eliminated using parametric methods, as evident from Figures 7, 9, and 10 for 0.5Cr0.5Mo0.25V steel. Moreover, the unknown curvatures of parametric plots limit extrapolation to three times the longest validated test figures available, so expensive and protracted test programs must be completed to obtain long-term design data.

In addition to highlighting the practical problems of acquiring long-term data, the results in Figures 7, 9, and 10 are of interest in relation to power-law descriptions of creep. Specifically, Eq. [3] indicates that failure times are governed by the rates of creep-strain accumulation. Yet, almost invariably, log σ/log t_f plots (Figure 9) and parametric plots (Figure 10) are presented as continuous curves. In contrast, because different creep mechanisms are believed to be dominant over successively higher stress ranges, log σ/log $\dot{\varepsilon}_m$ curves of the type shown in Figure 7 are traditionally represented as a connected series of tangents, *e.g.*, with $n \cong$ one, $n \cong 4$, and $n \gg 4$ before power-law breakdown occurs. Furthermore, the results in Figures 7, 9, and 10 curve continuously towards the ultimate tensile strength (UTS) value at the creep temperature, as would be expected because the UTS represents the upper stress limit of log σ/log $\dot{\varepsilon}_m$ and log σ/log t_f plots, making even the concept of power-law breakdown somewhat arbitrary.

VII. REPRESENTATION OF CREEP CURVE SHAPES

Progress in science is based on the premise that careful observations should lead to theories capable of prediction. Yet clearly, currently popular creep theories have not even led to theoretically justifiable methods for extrapolation of short-term data to obtain long-term property values. Moreover, the present analysis suggests that many of the key observations underpinning power-law creep approaches are questionable.

An obvious deficiency of traditional approaches is the assumption that normal curves can be adequately described by measuring only the "secondary" or steady-state creep rate, *i.e.*, the primary and tertiary stages are disregarded, so much of the information contained in a creep curve is ignored. In fact, inspection of constant-stress creep curves indicates that a steady-state condition is rarely achieved. Instead, with most metals and alloys, the decay in creep rate during the primary stage is offset by the acceleration associated with damage processes, such as the development of grain-boundary cavities and/or degradation processes, such as particle instability.

Thus, the secondary creep rate is often just a point of inflection, which can appear to be ostensibly constant over a limited strain range. It is, therefore, essential that comprehensive descriptions of the changes in creep strain rates with time and strain recognize that the dislocation configurations (and the particle morphologies and distributions in particle-hardened alloys) evolve during creep exposure, with these changes being material and exposure condition sensitive. For these reasons, the θ Projection Concept was introduced[38] in an effort to provide equations relating stress/strain/time/temperature in forms suitable for theoretical and practical purposes.

When creep takes place by diffusion-controlled generation and movement of dislocations, strain hardening occurs as the dislocation density increases with increasing primary strain. Simultaneously, recovery processes, such as climb and cross-slip, allow the dislocations to rearrange into low-energy configurations, so the dislocation distribution becomes less uniform as creep proceeds. Dislocations, therefore, experience a changing resistance to continued movement that depends on the local dislocation density, so the primary creep rate decays as the strengths of these barriers change due to strain hardening and recovery. Micromodeling of these processes leads to a description of primary creep in which the creep strain varies with time as

$$\varepsilon = \theta_1(1 - \exp(-\theta_2 t)) + \dot{\varepsilon}_s t \qquad [5]$$

where θ_1 scales the primary strain, θ_2 is a rate parameter governing the curvature of the primary stage, and $\dot{\varepsilon}_s$ is the steady-state creep rate eventually attained at long times.[19,36]

Equation [5] describes curves with a creep rate decaying gradually towards a steady-state value ($\dot{\varepsilon}_s$), as observed for aluminum (Figure 2). However, with most metals and alloys, a minimum rather than a steady creep rate occurs because the decaying primary rate is offset by the tertiary acceleration. Modeling of the intergranular damage and/or microstructural degradation processes causing tertiary creep then allows normal creep curves to be described[19,36] as

$$\varepsilon = \theta_1(1 - \exp(-\theta_2 t)) + \theta_3(\exp(\theta_4 t) - 1) \qquad [6]$$

where θ_3 scales the tertiary strain, and θ_4 is a rate parameter quantifying the tertiary curve shape. Equation 6 has been shown to provide accurate descriptions of the general shapes of normal curves. In addition, each θ parameter varies systematically with stress and temperature, representing the changes in creep-curve shape with changing test conditions. Thus, the θ relationships can quantify the observation that, particularly with particle-hardened alloys, the primary strain decreases with decreasing applied stress so that tertiary-dominated curves are usually displayed in tests of long duration.

In addition to allowing creep behavior patterns to be interpreted in terms of the processes controlling primary and tertiary creep, once the stress and temperature dependences of the θ parameters are established, quantities, such as $\dot{\varepsilon}_m$, can be computed in a manner that allows interpolation and extrapolation of data. Hence, for 0.5Cr0.5Mo0.25V ferritic steel,[38] analyses of creep curves obtained in tests with a maximum duration of ~1500 hours permit prediction of $\dot{\varepsilon}_m$ values at stresses giving creep lives in excess of 100,000 hours, with the results of independent test programs[46] confirming the accuracy of extrapolation (Figure 7).

The results in Figure 7 should also be considered on the basis that the extrapolation was carried out by analyzing curves recorded in high-stress tests (when $n \cong 12$), predicting the continuous curvature of the log σ/log $\dot{\varepsilon}_m$ plot so that n decreased gradually towards unity. Clearly, if different mechanisms controlled the creep properties exhibited within different stress/temperature regimes, analyzing data collected in one mechanism regime could not predict the behavior patterns in a different regime. The fact that the extrapolation is accurate then supports the view that the same dislocation process is dominant at all stress levels studied, *i.e.*, variations in n value are not a consequence of changes in the dominant creep mechanism.

In addition to quantifying creep parameters, the θ relationships allow prediction of creep rupture lives, *i.e.*, once the detailed shape of the creep strain/time curve is known, under uniaxial tension, the time to fracture (t_f) can be obtained as the time taken for the accumulated creep strain to reach the limiting creep ductility. The results presented in Figures 7 and 9 then show that accurate long-term estimates of both creep and stress rupture properties can be provided using the θ methodology. Moreover, the theoretically justifiable θ approach can be extended to quantify material behavior under the complex nonsteady stress-temperature conditions encountered in service applications,[47] offering full stress/strain/time/temperature relationships that can be expressed in computer-efficient forms suitable for use with the powerful finite-element packages now available for high-temperature design.

VIII. CONCLUSIONS

A basic premise of power-law creep approaches is that variations in n, m, and Q_c are a consequence of different mechanisms becoming dominant in different stress/temperature regimes. However, the log σ/log $\dot{\varepsilon}_m$ plots for aluminum, copper, and 0.5Cr0.5Mo0.25V steel can be well represented by continuous curves, with gradients decreasing from $n \gg 4$ near the UTS at the creep temperature towards $n \cong$ one at low stresses. Moreover, while the log σ/log $\dot{\varepsilon}_m$ relationships for aluminum appear to be grain-size independent over the range of grain diameters studied, this observation does not justify the common assumption that creep is grain-size insensitive (*i.e.*, $m \cong 0$) when dislocation processes are dominant. Thus, with materials, such as copper, the creep rates are shown to be grain-size dependent even when $n \geq 4$, so that $m \rightarrow 2$ or more as $n \rightarrow$ one with decreasing stress. This and much additional evidence then suggests that the dislocation processes controlling creep are essentially the same over the entire stress ranges covered not only for aluminum and copper but also for particle-hardened alloys, such as 0.5Cr0.5Mo0.25V steel.

The present analysis does not prove that creep can never occur by diffusional creep mechanisms, but certainly supports the view that measurements of n, m, and Q_c do not provide a reliable indication of the dominant creep process.[10] Moreover, despite being widely adopted for over 50 years, power-law concepts have not led to theories with verified predictive capabilities, so reliance must still be placed on empirical parametric methods in order to obtain long-term stress-rupture estimates. It is, therefore, proposed that power-law representation of steady-state creep rates should be abandoned in favor of approaches, such as the θ methodology, that seek to quantify the shapes of creep curves and the variations in curve shapes with changing test conditions. Creep behavior patterns can then be interpreted by distinguishing between the processes governing creep strain accumulation and the damage/degradation processes that usually cause the creep rates to accelerate into the tertiary stages preceding fracture, offering theoretically sound creep property descriptions capable of accurately predicting long-term design data for engineering materials.

REFERENCES

1. I.S. Servi and N.J. Grant: *J. Met.*, 1951, vol. 191, pp. 909-16.
2. J.G. Harper and J.E. Dorn: *Acta Metall.*, 1957, vol. 5, pp. 654-65.
3. J.G. Harper, L.A. Shepard, and J.E. Dorn: *Acta Metall.*, 1958, vol. 6, pp. 509-18.
4. C.R. Barrett, E.C. Muehleisen, and W.D. Nix: *Mater. Sci. Eng.*, 1972, vol. 10, pp. 33-42.
5. A.J. Ardell and S.S. Lee: *Acta Metall.*, 1986, vol. 34, pp. 2411-23.
6. H. Luthy, A.K. Miller, and O.D. Sherby: *Acta Metall.*, 1988, vol. 28, pp. 169-78.
7. J.D. Parker and B. Wilshire: *Phil. Mag.*, 1980, vol. 41, pp. 665-80.
8. E.H. Aigeltinger and R.C. Gifkins: *J. Mater. Sci.*, 1975, vol. 10, pp. 1889-1903.
9. O.A. Ruano, J. Wadsworth, and O.D. Sherby: *Acta Metall.*, 1988, vol. 36, pp. 1117-28.
10. B. Wilshire: *4th Int. Conf. on Creep and Fracture of Engineering Materials and Structures*, B. Wilshire and R.W. Evans, eds., The Institute of Materials, London, 1990, pp. 1-9.
11. B. Burton and G.L. Reynolds: *Mater. Sci. Eng.*, 1995, vol. A191, pp. 135-41.
12. G.L. Greenwood: *Creep Behaviour of Advanced Materials for the 21st Century*, R.S. Mishra, A.K. Mukherjee, and K.L. Murty, eds., TMS, Warrendale, PA, 1999, pp. 413-23.
13. J. Wadsworth, O.A. Ruano, and O.D. Sherby: *Creep Behaviour of Advanced Materials for the 21st Century*, R.S. Mishra, A.K. Mukherjee, and K.L. Murty, eds., TMS, Warrendale, PA, 1999, pp. 425-39.
14. B. Wilshire: *Creep Behaviour of Advanced Materials for the 21st Century*, R.S. Mishra, A.K. Mukherjee, and K.L. Murty, eds., TMS, Warrendale, PA, 1999, pp. 451-60.
15. K.R. McNee, G.W. Greenwood, and H. Jones: *Scripta Mater.*, 2001, vol. 44, pp. 351-57.

16. F.R.N. Nabarro: *Report on Conf. on Strength of Solids*, The Physical Society, London, 1948, pp. 75-87.
17. C. Herring: *J. Appl. Phys.*, 1950, vol. 21, pp. 437-45.
18. R.L. Coble: *J. Appl. Phys.*, 1963, vol. 34, pp. 1679-82.
19. R.W. Evans and B. Wilshire: *Creep of Metals and Alloys*, The Institute of Metals, London, 1985.
20. F.A. Mohamed and T.J. Ginter: *Acta Metall.*, 1982, vol. 30, pp. 1869-81.
21. B. Burton: *Phil. Mag.*, 1972, vol. 25, pp. 645-59.
22. W. Blum and W. Maier: *Phys. Status Solidi*, 1999, vol. 171a, pp. 467-74.
23. K.R. McNee, H. Jones, and G.W. Greenwood: *9th Int. Conf. on Creep and Fracture of Engineering Materials and Structures*, J.D. Parker, ed., The Institute of Materials, London, 2001, pp. 185-95.
24. B. Burton and G.W. Greenwood: *Met. Sci. J.*, 1970, vol. 4, pp. 215-18.
25. B. Burton and G.W. Greenwood: *Acta Metall.*, 1970, vol. 18, pp. 1237-42.
26. B. Wilshire and C.J. Palmer: *Scripta Mater.*, 2001, in press.
27. C.R. Barrett, J.L. Lytton, and O.D. Sherby: *Trans. AIME*, 1967, vol. 239, pp. 170-80.
28. E.R. Parker: *Trans. ASM*, 1958, vol. 50, pp. 52-104.
29. P. Feltham and J.D. Meakin: *Acta Metall.*, 1959, vol. 7, pp. 614-27.
30. Z. Kowalewski: *Arch. Met.*, 1992, vol. 37, pp. 65-76.
31. D. Hansen: *Trans. AIME*, 1939, vol. 133, pp. 15-57.
32. P. Shahinian and J.R. Lane: *Trans. ASM*, 1953, vol. 45, pp. 177-99.
33. F. Garofalo, W.F. Domis, and F. van Gemmingen: *Trans. TMS-AIME*, 1964, vol. 230, pp. 1460-67.
34. D.G. Morris: *Met. Sci. J.*, 1978, vol. 12, pp. 19-29.
35. S.L. Mannan and P. Rodriques: *Met. Sci. J.*, 1983, vol. 17, pp. 63-69.
36. R.W. Evans and B. Wilshire: *Introduction of Creep*, The Institute of Materials, London, 1993.
37. M. Pahutova, J. Cadek, and P. Rys: *Phil. Mag.*, 1971, vol. 23, pp. 509-17.
38. R.W. Evans, J.D. Parker, and B. Wilshire: *Recent Advances in Creep and Fracture of Engineering Materials and Structures*, B. Wilshire and D.R.J. Owen, eds., Pineridge Press, Swansea, 1982, pp. 135-84.
39. K.R. Williams and B. Wilshire: *Met. Sci. J.*, 1975, vol. 7, pp. 176-79.
40. J.D. Parker and B. Wilshire: *Met. Sci.*, 1975, vol. 9, pp. 248-52.
41. E. Arzt: *Res. Mech.*, 1991, vol. 31, pp. 399-453.
42. C.N. Ahlquist and W.D. Nix: *Acta Metall.*, 1971, vol. 19, pp. 373-85.
43. J.C. Gibeling and W.D. Nix: *Met. Sci. J.*, 1977, vol. 11, pp. 453-57.
44. M.E. Kassner: *Mater. Sci. Eng.*, 1993, vol. A166, pp. 81-88.
45. R.L. Orr, O.D. Sherby, and J.E. Dorn: *Trans. ASM.*, 1954, vol. 46, pp. 113-28.
46. R.J. Brown, B.J. Cane, J.D. Parker, and D.J. Walters: *Creep and Fracture of Engineering Materials and Structures*, B. Wilshire and D.R.J. Owen, eds., Pineridge Press, Swansea, 1981, pp. 645-57.
47. R.W. Evans and B. Wilshire: *Unified Constitutive Laws of Plastic Deformation*, A.S. Krausz and K. Krausz, eds., Academic Press, New York, NY, 1996, pp. 107-52.